Kinetic and Spectroscopic Studies of Hydrophilic Amino Acid Substitutions in the Hydrophobic Pocket of Human Carbonic Anhydrase II†

Joseph F. Krebs,‡,§ Fazale Rana,‖ Richard A. Dluhy,‖ and Carol A. Fierke*,‡

Department of Biochemistry, Duke University Medical Center, Box 3711, Durham, North Carolina 27710, and Department of Chemistry, University of Georgia, Athens, Georgia 30602

Received November 25, 1992

ABSTRACT: The functional importance and structural determinants of a conserved hydrophobic pocket in human carbonic anhydrase II (CA II) were probed by preparing and characterizing 13 amino acid substitutions at Leu-198, situated at the mouth of the pocket. The pH dependence of the esterase activity reveals that activity decreases (up to 120-fold) as the amino acid size and charge at position 198 are varied while the pK_a of the zinc-bound water molecule increases (up to 1 pH unit). Intriguingly, the pH dependence of the Leu-198→Glu substitution is parabolic (pK_as ≈ 6 and 9), consistent with introduction of a general base-catalyzed mechanism. Kinetic characterization of CO_2/HCO_3^- interconversion catalyzed by four variants (Leu-198→Ala, His, Arg, and Glu) reveals that increasing the size of the hydrophobic pocket (Ala) does not compromise catalysis (≈3-fold decrease); however, substitution of charged (Arg and Glu) and larger (His) amino acids decreases k_{cat}/K_M for CO_2 hydration substantially (17-fold, 19-fold, and 10-fold, respectively) but not completely. log k_{cat}/K_M for CO_2 hydration, HCO_3^- dehydration, and *p*-nitrophenyl acetate hydrolysis correlates with the hydrophobicity of the residue at 198, likely reflecting desolvation or electrostatic destabilization of the ground state. The X-ray crystal structures of the Leu-198→His, Glu, and Arg variants (Nair & Christianson, 1993) indicate that the His and Glu side chains are accommodated by minor structural reorganization leading to a wider mouth for the hydrophobic pocket while the Arg side chain blocks the pocket. Infrared spectroscopy of CO_2 bound to either wild-type CA II or the Leu-198→Arg variant indicates that the Arg substitution both decreases the affinity and alters the position of CO_2 binding, suggesting that the hydrophobic pocket forms the CO_2 binding site in CA II. Finally, a 1.5-fold increase (Leu-198→Ala) and 12-fold decrease (Leu-198→Arg) in k_{cat} for CO_2 hydration, indicative of the rate constant for intramolecular proton transfer from zinc-bound water to His-64, are likely mediated by changes in the active site solvent structure.

Carbonic anhydrase is a zinc metalloenzyme which efficiently catalyzes the hydration of CO_2 to form bicarbonate and a proton. Catalysis of CO_2 hydration by one isozyme, human carbonic anhydrase II (CA II,[1] EC 4.2.1.1), approaches the diffusion-control limit at 10^8 M^{-1} s^{-1} and has a maximum turnover rate of more than 10^6 per second [for recent reviews, see Silverman and Lindskog (1988) and Christianson (1991)]. CA II also catalyzes the hydrolysis of aromatic esters and is potently inhibited by sulfonamide compounds and monovalent anions.

A crystal structure of CA II has been solved (Liljas et al., 1972) and refined (Eriksson et al., 1986, 1988; Håkansson et al., 1992) to 1.54-Å resolution, providing tremendous insights into structure–function relationships within the enzyme. The zinc cofactor lies at the base of the conical active site cleft where it is coordinated to three histidine residues and a solvent molecule in a tetrahedral geometry. The zinc-bound hydroxide acts as a nucleophile to catalyze CO_2 hydration and ester hydrolysis (Coleman, 1967; Lindskog & Coleman, 1973). Catalysis of CO_2 hydration occurs in two steps: CO_2/HCO_3^- interconversion generating a zinc-bound water intermediate followed by regeneration of the zinc hydroxide species by proton transfer to solvent using the active site residue His-64 as a proton shuttle (Steiner et al., 1975; Tu et al., 1989).

The active site cleft is split into hydrophobic and hydrophilic regions; the side chains of Val-121, Val-143, Leu-198, and Trp-209 form a hydrophobic pocket adjacent to the zinc hydroxyl group, as shown in Figure 1 (Eriksson et al., 1986, 1988). Infrared spectroscopy (Riepe & Wang, 1968) and theoretical studies (Merz, 1990, 1991; Liang & Lipscomb, 1990) have implicated this pocket in CO_2 binding. This site is consistent with a variety of spectroscopic studies [for example, Bertini et al. (1983, 1987) and Williams and Henkens (1985)], suggesting that CO_2 binding does not involve inner-sphere coordination with zinc. Structure–function studies in the hydrophobic pocket at Val-121 (Nair et al., 1991) and Val-143 (Fierke et al., 1991; Alexander et al., 1991) indicate that the hydrophobicity of this pocket is important for the stabilization of the transition state for CO_2 hydration and ester hydrolysis. Random mutagenesis studies of the Asp-190–Ile-210 region of human CA II indicate that substitution of Arg or Pro at position 198 decreases catalytic activity and sulfonamide binding (Krebs & Fierke, 1993). A leucine side chain is found at this position for all CA I and CA II isozymes while phenylalanine is present in CA III isozymes (Hewett-

† Supported by National Institutes of Health Grants GM40602 (C.A.F.) and GM40117 (R.A.D.). C.A.F. received an American Heart Association Established Investigator Award and a David and Lucile Packard Foundation Fellowship in Science and Engineering.

* Corresponding author.

‡ Duke University Medical Center.

§ Current address: Department of Molecular Biology, Scripps Research Institute, Room MB103, 10666 N. Torrey Pines Road, La Jolla, CA 92037.

‖ University of Georgia.

[1] Abbreviations: CA II, human carbonic anhydrase II; Tris, tris(hydroxymethyl)aminomethane; EDTA, (ethylenedinitrilo)tetraacetic acid; MES, 2-(*N*-morpholino)ethanesulfonic acid; CHES, 2-(*N*-cyclohexylamino)ethanesulfonic acid; MOPS, 3-(*N*-morpholino)propanesulfonic acid; IR, infrared; BCA, bovine carbonic anhydrase; PNPA, *p*-nitrophenyl acetate. Enzyme variants are designated in the following way: wild-type amino acid number → substituted amino acid.

0006-2960/93/0432-4496$04.00/0

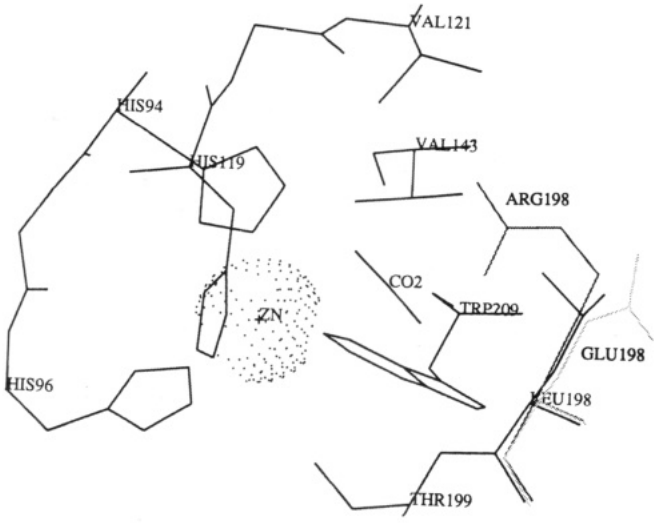

FIGURE 1: Structure of the hydrophobic pocket in the active site of recombinant human carbonic anhydrase II taken from the X-ray crystal structure of Alexander et al. (1991) showing the zinc coordinated to three imidazole ligands, His-94, His-96, and His-119; four amino acids defining the hydrophobic pocket, Val-121, Val-143, Leu-198, and Trp-209; and an essential catalytic residue, Thr-199. The position of the substituted amino acid for Leu-198→Arg and Leu-198→Glu CA II is taken from the X-ray crystal structures of these variants (Nair & Christianson, 1993). The position of CO_2 was determined from a least-squares superposition of the backbone atoms of CA II with the calculated CA II–CO_2 complex (Merz 1990, 1991).

Emmett & Tashian, 1991); this structural difference is proposed to be a key determinant of the catalytic properties of CA III (Eriksson et al., 1988; LoGrasso et al., 1991).

To further probe the structure–function relationships within the CA II active site, 13 substitutions in Leu-198 at the mouth of the hydrophobic pocket were created and their hydrase and esterase activities determined. The properties of four variants, including truncation of the side chain (Ala) and substitution with charged (Arg and Glu) and larger (His) amino acids, were determined using spectroscopic and steady-state kinetic techniques. The Leu-198→Arg substitution alters the position of bound CO_2 as assayed by the infrared spectrum of CO_2, such that it does not overlap with bound azide, an active site inhibitor, as observed for wild type. A correlation between hydrophobicity and log k_{cat}/K_M for CO_2 hydration, HCO_3^- dehydration, and *p*-nitrophenyl acetate hydrolysis indicates that charge delocalization occurs in the chemical transition state. However, catalysis is not abolished by radical substitutions; this can be understood in light of the crystal structures of these variants (Nair & Christianson, 1993).

MATERIALS AND METHODS

Mutagenesis. Oligonucleotide-directed mutagenesis of the cloned CA II gene in plasmid pCAM-a1 (Krebs & Fierke, 1993) was performed according to the method of Stannsens et al. (1989) using T4 DNA polymerase and *Escherichia coli* DNA ligase with a 25-base oligonucleotide in which the Leu-198 codon (CTG) was replaced by a degenerate codon (an equimolar mixture of all four bases). The resulting DNA was first transformed into WK6 mutS and then into BL21-(DE3) pLysS using the procedure of Hanahan (1983). Colonies with plasmids encoding mutant CA II were identified using esterase and sulfonamide binding activity screens (Krebs & Fierke, 1993). The entire DNA sequence of the CA II gene was determined by the method of Sanger (1977) for each mutant candidate prior to purification.

Protein Expression and Purification. BL21 (DE3) pLysS cells (Studier & Moffat, 1986) containing pCAM-a1 encoding either wild-type or mutant CA II were grown, and CA II was induced by addition of 1 mM isopropyl β-D-thiogalactopyranoside and 0.3 mM $ZnSO_4$ followed by incubation at 31–34 °C for 5–6 h. Cells were pelleted, and a crude lysate was prepared by EDTA/lysozyme lysis followed by removal of cellular remnants by centrifugation (20000*g*, 20 min) (Krebs et al., 1991). Leu-198 variants were purified from these cell extracts using sulfonamide affinity chromatography at pH 8.0 (Osborne & Tashian, 1975). Protein samples were then extensively dialyzed against 5 mM potassium phosphate buffer (pH 7.5), lyophilized, and stored at –20 °C.

Esterase and CO_2 Hydration Assays. The specific activity for *p*-nitrophenyl acetate (PNPA) hydrolysis in cell extracts was determined at 25 °C at 0.5 mM PNPA (0.1 M Tris–SO_4, 5% acetone, pH 8.0, I = 0.2 with Na_2SO_4), by measuring the change in A_{348}/min (ϵ_{348} = 5000 M^{-1} cm^{-1}) (Armstrong et al., 1966). The pH dependence of esterase activity was measured in 50 mM Na-MES (5.5–7.0), Tris–SO_4 (7.5–9.0), or Na-CHES (9.0–10.0) buffer with the ionic strength adjusted to 0.1 M using sodium sulfate. The apparent second-order rate constants, $(k_{cat}/K_M)_{obs}$, were calculated from initial rates after subtraction of the acetazolamide-inhibited rates. The concentration of CA II was determined either by stoichiometric titration of esterase activity using acetazolamide (Pocker & Stone, 1967) or from absorbance using ϵ_{280} = 5.4 × 10^4 M^{-1} cm^{-1} (Tu & Silverman, 1982). The pH-independent rate constant, k_{cat}/K_M, and the catalytic pK_a were determined by fitting the observed pH dependence of esterase activity to either eq 1 or eq 2 (Leu-198→Glu) using the curve-fitting program SYSTAT (Systat, Inc).

$$(k_{cat}/K_M)_{obs} = (k_{cat}/K_M)/(1 + 10^{pK_a - pH}) \quad (1)$$

$$(k_{cat}/K_M)_{obs} = (k_{cat}/K_M)/(1 + 10^{pK_{a1} - pH} + 10^{pH - pK_{a2}}) \quad (2)$$

CO_2 Hydration and Bicarbonate Dehydration. The CO_2 hydration activity of each variant was measured in cell extracts by the pH-indicator assay of Brion et al. (1988) at 2 °C in 20 mM imidazole, 5 mM Tris–SO_4, and 0.2 mM *p*-nitrophenol. Initial rates of CO_2 hydration and bicarbonate dehydration were measured in a Kin-Tek stopped-flow apparatus at 25 °C by the changing pH-indicator method (Khalifah, 1971). Buffer/indicator pairs (with the wavelengths observed) were MES/chlorophenol red (pH 6.1, 574 nm), MOPS/*p*-nitrophenol (pH 6.7–7.7, 407 nm), and TAPS/*m*-cresol purple (pH 8.3–8.9, 578 nm). The buffer concentration was either 50 mM (CO_2 hydration) or 100 mM (bicarbonate dehydration) with the ionic strength adjusted to 0.1 M with sodium sulfate and 0.1 mM EDTA added to prevent inhibition by metal ions. The assay was initiated by a 2:5 dilution of CA II (10 nM–20 μM final concentration) into substrate (either 3–27 mM CO_2 or 4–200 mM HCO_3^-). Solvent isotope effects were measured using identical substrate and buffer/indicator solutions prepared with 99.9% D_2O. The solution pD was determined by adding 0.4 to the pH meter reading (Glasoe & Long, 1960).

Infrared (IR) Spectroscopy. Enzyme samples were prepared for IR spectroscopic analysis by dissolving lyophilized CA II (100–150 mg) in 10 mM Tris–SO_4, pH 8.0, 4 °C. In one series of experiments, solid ethoxzolamide was added to the samples to act as an inhibitor. CA II was then dialyzed against 10 mM MES, pH 5.5 (2×), followed by 0.25 mM MES, pH 5.5 (2×, either with or without 10 μM ethoxzolamide), and relyophilized. Before the IR spectrum was

obtained, the enzyme samples were redissolved in 1 mM MES, pH 5.5, with or without 10 mM sodium azide, to a protein concentration of 6–9 mM. The samples were equilibrated at room temperature for a minimum of 2 h with defined mixtures of CO_2/N_2 in a glove bag and stored in equilibrated gas-tight vials.

Aliquots of the enzyme–CO_2 sample were removed from the sample vials using a 0.1-mL Hamilton syringe; the enzyme solutions were then loaded onto a demountable IR transmission cell equipped with CaF_2 windows and 12-μm spacers (Harrick Scientific, Ossining, NY). Transmission infrared spectra of the enzyme–CO_2 samples were obtained using a Digilab FTS-60 Fourier transform infrared spectrometer (Bio-Rad, Digilab Division, Cambridge, MA) equipped with a narrow-band, liquid N_2-cooled HgCdTe detector (Infrared Associates, Orlando, FL) at 2-cm^{-1} resolution with triangular apodization and one level of zero filling. In order to eliminate any extraneous CO_2 of atmospheric origin from the spectrometer's optical path, the entire spectrometer (including optical bench, sample chamber, and interferometer air bearing) was purged with pure N_2 gas (obtained from the boil-off of a high-pressure, liquid N_2 tank) for approximately 12 h before data collection began. In addition, after the samples were changed, the sample chamber of the spectrometer (which can be sealed off from the main optical bench) was further purged for at least 10 min prior to data collection. Absorbance spectra were obtained by ratioing the single-beam IR spectrum of the enzyme–CO_2 complex to that of an empty cell background. Typically, 256 scans were collected to improve the signal-to-noise ratio in the final spectra. The IR spectra presented here have been baseline corrected but have not been smoothed. Vibrational wavenumber positions were calculated using a center of gravity algorithm (Cameron et al., 1983) and are accurate to better than ± 0.1 cm^{-1}. For each individual sample, carbonic anhydrase activity and protein concentration were measured on the material recovered from the transmission cell after measurement of the IR spectra.

CO_2 difference spectra were obtained by subtraction of the spectrum of freely dissolved CO_2 in aqueous solution from the spectrum of CO_2 in the presence of the inhibited or uninhibited enzyme. The relative levels of enzyme-bound and free CO_2 were determined from the integrated intensities of the CO_2 difference spectrum and the corresponding total CO_2 spectrum after correction for the bound CO_2 component. The integrated intensity of the protein amide III band between 1355 and 1205 cm^{-1} in combination with UV absorbance values at 280 nm was used to normalize the integrated intensities of the total and bound CO_2 in order to correct for minor differences in path length and protein concentration. Spectral data files were downloaded from the spectrometer's dedicated computer to an IBM-type personal computer for further data analysis. Integrated peak areas were determined using the program LabCalc (Galactic Industries, Nashua, NH). The relative levels of enzyme-bound and free CO_2 were determined from the peak areas of the CO_2 difference spectrum and the corresponding total CO_2 peak. The fraction of enzyme containing bound CO_2, X_{bound}, was determined from the normalized, relative integrated areas of the bound and free CO_2 peaks:

$$X_{bound} = ([CO_2]_{bound}/[CO_2]_{total})/[E]_{total} \quad (3)$$

where $[E]_{total}$ is the total concentration of enzyme in the sample.

RESULTS

Activity Screen. The PNPA esterase and CO_2 hydrase activity of 13 variants at Leu-198 (Table I) were measured as a preliminary characterization of the functional consequences of substitution at this site. The esterase activity was measured under k_{cat}/K_M conditions (0.5 mM PNPA), and the hydrase activity was determined using a qualitative pH-indicator assay (Brion et al., 1988) at an initial CO_2 concentration of 38 mM (k_{cat} conditions for wild-type enzyme). Conservative substitutions (Met, Cys) have little effect on catalytic activity; however, substitutions which vary the size (Trp and Gly), hydrophobicity (Ser and His), or charge (Arg, Lys, Asp, and Glu) decrease both esterase and hydrase activity significantly but not completely. Insertion of negative charge (Asp and Glu) at this position decreases esterase activity more than additional positive charge (Arg and Lys). The catalytic pK_a, estimated from the ratio of the esterase activity at pH 8.0 and 6.5, is not affected by uncharged substitutions (data not shown).

Table I: Hydrase and Esterase Activity of CA II Variants at Leu-198[a]

variant	PNPA hydrolysis[b] (M^{-1} s^{-1})	CO_2 hydrase activity[c] (relative to wild type)
wild type	2500[d]	1.0[d]
Leu-198 → Met	3500[d]	1.3[d]
Leu-198 → Cys	3300	1.1
Leu-198 → Ala	340	1.2
Leu-198 → Gly	820	0.11
Leu-198 → Arg	680[d]	0.02[d]
Leu-198 → Val	360	0.92
Leu-198 → His	300	0.13
Leu-198 → Pro	180[d]	0.04[d]
Leu-198 → Lys	140	0.16
Leu-198 → Trp	100	0.27
Leu-198 → Ser	60	0.23
Leu-198 → Glu	20	0.07
Leu-198 → Asp	20	

[a] Specific activity of CA II measured in crude cellular lysates. [b] Measured at 0.5 mM PNPA and 0.1 M Tris–SO_4, pH 8.0, $I = 0.2$ with sodium sulfate, 25 °C. [c] Assayed at 2 °C using imidazole/*p*-nitrophenol as the buffer/indicator pair (Brion et al., 1988). [d] Taken from Krebs and Fierke (1993).

Esterase Activity. To further examine the structural requirements of this region of the hydrophobic pocket, the catalytic properties of four Leu-198 variants (Leu-198→Ala, Arg, Glu, and His), including truncation of the side chain and charge substitution, were determined in detail. The pH dependence of $(k_{cat}/K_M)_{obs}$ for PNPA hydrolysis was measured (Figure 2). The decrease in esterase activity was time-independent, indicating that it was not due to enzyme instability. With the exception of the Leu-198→Glu mutant, the pH dependence of esterase activity is consistent with the ionization of a single enzymic group; the pH-independent rate constant, k_{cat}/K_M, and the pK_a for esterase activity are listed in Table II. For wild-type CA II this pK_a is proposed to reflect the ionization of the catalytically important zinc–water ligand (Lindskog, 1966). The pH dependence of the Leu-198→Glu mutant has a parabolic shape (Figure 2), consistent with a model in which esterase activity is dependent on the ionization of two distinct groups (described by eq 2), where inactive enzyme species are formed at low and high pH.

CO_2 Hydration and HCO_3^- Dehydration. The pH dependence of the CO_2 hydration activity of Leu-198 variants (Table III) was measured using the pH-indicator method of Khalifah (1971). Michaelis–Menten kinetic behavior was observed for all variants. $k_{cat}^{CO_2}/K_M$ decreases 3-fold for truncation of the side chain (Ala) and 17–19-fold for insertion of a charged amino acid. For wild-type CA II, the pH dependence for $k_{cat}^{CO_2}/K_M$ and $k_{cat}^{CO_2}$ is consistent with the ionization of a single group with a pK_a near 7.1 and 7.4, respectively (Steiner

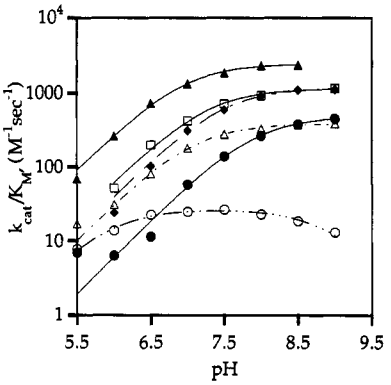

FIGURE 2: pH dependence of k_{cat}/K_M for PNPA esterase activity for Leu-198 variants, wild type (▲), Leu-198→Gly (□), Leu-198→Arg (◆), Leu-198→Ala (△), Leu-198→His (●), and Leu-198→Glu (○), measured at 0.5 mM PNPA and 50 mM buffer, 25 °C, with the ionic strength maintained at 0.1 with sodium sulfate. The lines were fit to the data using either eq 1 or eq 2 (Leu-198→Glu) with the curve-fitting program SYSTAT using the kinetic parameters listed in Table II.

Table II: pH Dependence of Esterase Activity[a]

variant	k_{cat}/K_M[b] (M^{-1} s^{-1})	pK_a[b] measured	pK_a[c] calculated
wild type	2680 ± 80	6.93 ± 0.05	7.3
Leu-198 → Ala	390 ± 10	7.07 ± 0.03	7.1
Leu-198 → Arg	940 ± 10	7.48 ± 0.03	7.3
Leu-198 → Gly	840 ± 20	7.25 ± 0.04	
Leu-198 → His	520 ± 6	7.90 ± 0.02	7.1
Leu-198 → Glu	27 ± 1	5.92 ± 0.07	6.9
		8.92 ± 0.06	

[a] The PNPA esterase activity was measured as described for Figure 1. [b] The pH-independent rate constant for PNPA esterase activity, k_{cat}/K_M, the observed pK_a, and the standard error were calculated from a nonlinear least-squares fit of the data using SYSTAT with eq 1 or 2 (Leu-198 → Glu). [c] The pK_a was calculated using the Haldane relation (eq 4) from the ratio of k_{cat}/K_M for CO_2 hydration at pH 6.1 and HCO_3^- dehydration at pH 8.9.

et al., 1975). The observed pH dependence of $k_{cat}^{CO_2}/K_M$ for Leu-198→Ala and Leu-198→His variants is similar, suggestive of a pK_a near 7, while $k_{cat}^{CO_2}/K_M$ for Leu-198→Arg and Leu-198→Glu enzymes is roughly pH independent in this region. However, $k_{cat}^{CO_2}$ for the Leu-198 variants increases 3–10-fold when the pH is increased from 7.1 to 8.9, suggesting that the pK_a for this parameter is >7.4. The pH dependence of $k_{cat}^{CO_2}/K_M$ for Leu-198→Glu CA II is not bell-shaped, as observed for esterase activity.

The kinetic parameters for HCO_3^- dehydration catalyzed by Leu-198 variants were measured at pH 6.1, varying the HCO_3^- concentration in the range 4–200 mM, as shown in Table IV. Under these conditions all variants exhibited Michaelis–Menten kinetic behavior. Since pH 6.1 is well below the observed pK_a, the majority of the enzyme should be in the catalytically active form. Substitutions at position 198 cause minor decreases in $k_{cat}^{HCO_3^-}/K_M$ (2–15-fold), as observed for CO_2 hydration. However, the Leu-198→Arg substitution significantly lowers $k_{cat}^{HCO_3^-}$ (89-fold).

To check the accuracy of the pH-independent k_{cat}/K_M for CO_2 hydration and HCO_3^- dehydration estimated from the data at pH 8.9 and 6.1, respectively, the pK_a of the zinc–water group was calculated for each variant using the Haldane relation (Segel, 1975) shown in the equation:

$$K_a^{H_2CO_3}/K_a^{ZnH_2O} = (k_{cat}^{CO_2}/K_M)/(k_{cat}^{HCO_3^-}/K_M) \quad (4)$$

where $K_a^{H_2CO_3}$ is the apparent dissociation constant for H_2CO_3 ($\approx 6.3 \times 10^{-7}$ M) (Steiner et al., 1975). There is good agreement between the calculated zinc–water pK_as (Table II) and those measured using esterase activity, with the exception of Leu-198→His and Leu-198→Glu. Therefore, for these variants either the pH dependence of esterase activity does not directly reflect the ionization of the zinc–water species or the estimated limiting values are incorrect.

To determine if a proton transfer is occurring in the rate-limiting step, the solvent deuterium isotope effects on the steady-state kinetic parameters for CO_2 hydration at pD 8.9 and HCO_3^- dehydration at pD 6.1 were also measured (Tables III and IV). Since these pHs are significantly distant from the observed pK_as (with the possible exception of Leu-198→Glu), the isotope effects should be derived primarily from kinetic rather than equilibrium isotope effects (Showen, 1977). No significant isotope effect is observed in k_{cat}/K_M in either direction for the majority of Leu-198 substitutions, indicating that the rate-limiting step under these conditions does not involve a proton transfer. However, a solvent isotope effect of 3.2 is observed in k_{cat}/K_M for HCO_3^- dehydration catalyzed by the Leu-198→Ala mutant, suggesting that a proton transfer is partially rate-limiting. An isotope effect on $k_{cat}^{CO_2}$ for CO_2 hydration is observed for wild-type CA II, indicative of rate-limiting proton transfer from the zinc–solvent molecule to His-64 (Steiner et al., 1975; Tu et al., 1989); this isotope effect is retained for all Leu-198 substitutions. In the reverse direction, a solvent isotope effect in $k_{cat}^{HCO_3^-}$ is observed for both wild-type and Leu-198→Ala enzymes, reflecting intramolecular proton transfer, but the isotope effect is decreased for the Arg and Glu substitutions, indicating a novel rate-limiting step.

IR Spectroscopy. Although the intense IR absorbance of water makes IR studies in aqueous solutions problematic, freely dissolved CO_2 absorbs at 2343.5 cm^{-1}, a frequency which occurs in a spectral region otherwise devoid of vibrational bands due to the protein and most other organic molecules, thus making this region of the spectrum ideal for the study of bound ligands to the active site of CA II (D'Esposito & Koenig, 1978; Thomas & Kyogoku, 1977). In dissolved aqueous solution, the CO_2 vibration occurs on the shoulder of the so-called "water association" band centered around 2100 cm^{-1} (Cameron et al., 1979). However, simple spectral subtraction of the underlying H_2O band is sufficient to accurately calculate the frequency, bandwidth, and area of the CO_2 vibration (Figure 3B).

The CO_2 IR band at 2343 cm^{-1} is derived from the asymmetric stretching vibration of the CO_2 molecule, a vibrational mode which is particularly sensitive to solvent polarity (Riepe & Wang, 1968). To examine the interactions between CO_2 and CA II, the pH of the solution must be less than the apparent pK_a of HCO_3^- (6.2) so the equilibrium will favor the formation of CO_2. Both wild-type and mutant enzymes are stable at low pH; no significant decline in esterase activity is observed when the enzyme is incubated at pH 5.5 for >2 h. Furthermore, only small decreases in activity (<20%) are observed after exposure to the IR beam path under experimental conditions. Addition of azide or ethoxzolamide completely inhibits the observed esterase activity.

The equilibration of atmospheric CO_2 gas (P_{CO_2} = 1 atm) with a solution of CA II (7–17 mM in 1 mM MES, pH 5.5) results in a slight shift of the frequency of the overall CO_2 band shape to a lower wavenumber (center of gravity = 2342.5 cm^{-1}) (Figure 3A). A frequency shift of this magnitude and direction has also been observed in the IR spectrum of bovine carbonic anhydrase equilibrated with CO_2 (Riepe & Wang, 1968). Spectral analysis of the CO_2 peak using deconvolution

Table III: pH Dependence of Steady-State Kinetic Parameters for CO_2 Hydration of CA II Variants at Leu-198[a]

parameter	pH	amino acid at position 198				
		Leu	Ala	His	Glu	Arg
k_{cat}/K_M (μM^{-1} s^{-1})	7.1	67 ± 3	25 ± 3	5.3 ± 0.6	2.7 ± 0.3	8.7 ± 1
	7.7	80 ± 6			3.2 ± 0.2	12 ± 1
	8.9	120 ± 2	35 ± 10	12 ± 3	6.3 ± 0.3	7.1 ± 0.6
k_{cat} (ms^{-1})	7.1	400 ± 10	160 ± 10	48 ± 2	120 ± 30	23 ● 2
	7.7	630 ± 30			130 ± 10	39 ± 6
	8.9	980 ± 100	1600 ± 300	270 ± 40	330 ± 50	78 ± 3
K_M (mM)	7.1	6.0 ± 0.3	6.3 ± 0.7	8.9 ± 1	44 ± 15	2.6 ± 0.3
	7.7	8.0 ± 1			41 ± 16	3.3 ± 0.2
	8.9	8.6 ± 2	46 ± 13	23 ± 5	54 ± 11	11 ± 1
$(k_{cat}/K_M)^H/(k_{cat}/K_M)^D$ [b]	8.9	1.1 ± 0.2	1.0 ± 0.2		1.3 ± 0.1	1.0 ± 0.2
k_{cat}^H/k_{cat}^D [b]	8.9	4.0 ± 0.3	6.5 ± 1.6		2.7 ± 0.5	4.0 ± 0.5

[a] Activity measured as a function of [CO_2] in 50 mM buffer, 25 °C, I = 0.1 with sodium sulfate, using a pH-indicator assay (Khalifah, 1971). [b] k^D measured in 99.9% D_2O.

Table IV: Steady-State Kinetic Parameters for HCO_3^- Dehydration of CA II Variants at Leu-198[a]

variant	k_{cat}/K_M		k_{cat}		K_M (mM)
	μM^{-1} s^{-1}	k^H/k^D [b]	ms^{-1}	k^H/k^D [b]	
wild type	9.4 ± 1	1.0 ± 0.4	720 ± 80	3.9 ± 0.8	77 ± 10
Leu-198 → Ala	4.8 ± 0.5	3.2 ± 0.6	450 ± 60	2.7 ± 0.7	95 ± 20
Leu-198 → His	1.5 ± 0.2		130 ± 20		85 ± 30
Leu-198 → Glu	1.1 ± 0.06	1.0 ± 0.1	170 ± 30	1.2 ± 0.2	160 ± 40
Leu-198 → Arg	0.63 ± 0.08	1.4 ± 0.4	8.1 ± 0.4	1.1 ± 0.2	13 ± 2

[a] Activity measured as a function of [HCO_3^-] in 50 mM MES, pH 6.1, 25 °C, I = 0.1 with sodium sulfate, using a pH-indicator assay (Khalifah, 1971). [b] k^D measured in 99.9% D_2O.

or derivative techniques reveals that this band is actually composed of two overlapping IR vibrations centered at 2353.5 and 2340 cm^{-1} (data not shown). The band at 2343.5 cm^{-1} is due to dissolved CO_2 gas in solution, as discussed previously. We have found that the frequency, intensity, or half-width of the band due to freely dissolved CO_2 gas is not affected by the presence of buffer or inhibitors in solution. Therefore, the new vibration at 2340 cm^{-1} can be attributed to the binding of CO_2 by the enzyme. The binding of CO_2 by CA II results in a vibrational frequency for the bound CO_2 species which is shifted slightly to lower wavenumbers compared to the freely dissolved CO_2 gas, indicating a more hydrophobic environment for the bound ligand compared with the dissolved gas. The bound CO_2 band is clearly observed in the spectrum of CO_2 in the presence of CA II when the spectrum of freely dissolved CO_2 gas in solution is subtracted from that of [CO_2 + CA II] (Figure 3C).

We have also obtained the IR spectrum of the wild-type CA II enzyme in a solution equilibrated with CO_2 (P_{CO_2} = 1 atm) and the enzyme inhibitor ethoxzolamide. The IR spectrum of a solution of [CO_2 + CA II + ethoxzolamide] reveals a CO_2 band whose peak position (≈2343.5 cm^{-1}) and band parameters are similar to that of freely dissolved CO_2 (Figure 3D). Deconvolution and derivative analysis of this spectrum suggest that the CO_2 band in the enzyme–inhibitor sample is composed of only a single component. Subtraction of the spectrum of freely dissolved CO_2 gas from the spectrum of [CO_2 + CA II + ethoxzolamide] reveals no new bands shifted to lower frequency (Figure 3E), but only a small residual intensity attributed to free CO_2 gas. A similar result is obtained when CO_2 is equilibrated with CA II and the enzyme inhibitor sodium azide (data not shown); that is, subtraction of free CO_2 from [CO_2 + CA II + azide] does not result in any additional peak attributable to a bound CO_2 species. Since both ethoxzolamide and azide bind to the zinc cofactor, these results provide additional evidence that the difference band at 2340 cm^{-1} is due to the specific interaction of CO_2 with the enzyme active site. The intensity of the bound CO_2 band (as assayed from the [CO_2 + CA II] − [CO_2] difference peak at 2340 cm^{-1}) increases roughly as the CO_2 concentration increases. Assuming a single binding site, the fraction of enzyme containing bound CO_2 (X_{bound}, eq 3) as a function of CO_2 concentration is consistent with the dissociation constant for CO_2 of 0.1 M measured by Riepe and Wang (1968) for the BCA–CO_2 complex.

The binding of CO_2 to the Leu-198→Arg variant of CA II was also studied. We have observed a CO_2 peak at 2343 cm^{-1} in the IR spectrum of the Leu-198→Arg variant equilibrated with CO_2 in a 100% CO_2 atmosphere (P_{CO_2} = 1 atm) (Figure 4A). When the IR spectrum of freely dissolved CO_2 was subtracted from the spectrum of [CO_2 + Leu-198→Arg CA II], a significant difference peak was observed at 2341 cm^{-1} (Figure 4B). However, unlike the case of the wild-type enzyme, we also observe a significant difference peak at 2341 cm^{-1} when the spectrum of free CO_2 is subtracted from the spectrum of CO_2 in the presence of Leu-198→Arg CA II and inhibitor. Figure 4D shows the difference spectrum which results when the spectrum of freely dissolved CO_2 is subtracted from the spectrum of [CO_2 + Leu-198→Arg CA II + azide]. This suggests that the difference peak at 2341 cm^{-1} is derived from a CO_2 species interacting with the enzyme outside the active site. The intensity of the bound CO_2 difference peak at 2341 cm^{-1} in the Leu-198→Arg CA II variant is smaller than the intensity of the bound CO_2 difference peak in the wild-type CA II, which would be consistent with an increased K_D for CO_2 binding to this variant.

DISCUSSION

In the current study the plasticity of a hydrophobic pocket in CA II was probed by catalytic, spectroscopic, and crystallographic (Nair & Christianson, 1993) studies of substitutions at Leu-198. Structure–function (Krebs & Fierke, 1993; Fierke et al., 1991; Nair et al., 1991; Alexander et al., 1991; LoGrasso et al., 1991, 1993), spectroscopic (Riepe & Wang, 1968), theoretical (Merz, 1990, 1991; Liang &

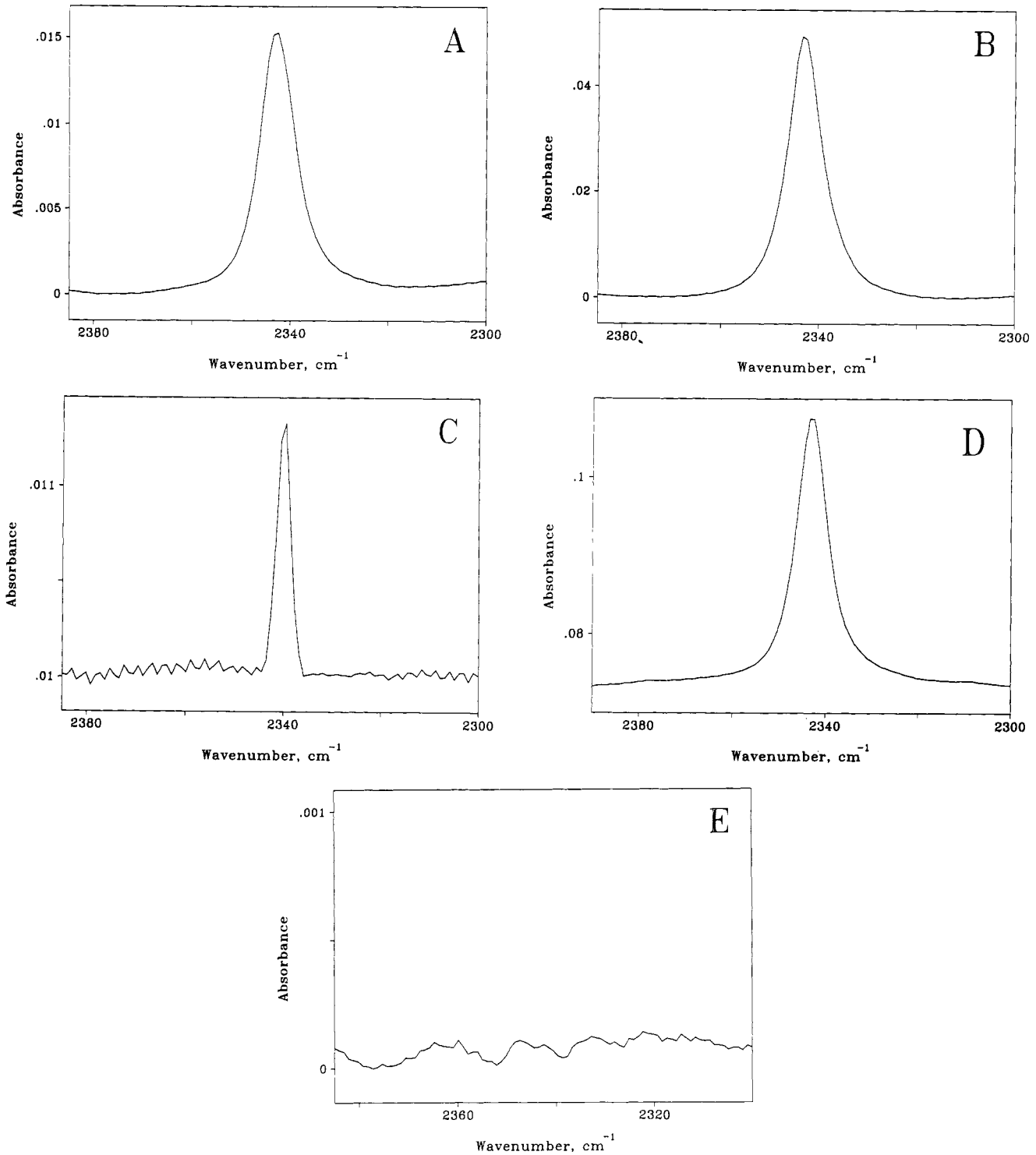

FIGURE 3: Infrared spectra of the asymmetric CO_2 stretching vibration obtained by dissolving CO_2 gas (P_{CO_2} = 1 atm) in 0.25 mM MES, pH 5.5, in the presence of wild-type CA II. (A) Spectrum of CO_2 in solution in the presence of 7.5 mM wild-type CA II. (B) Spectrum of freely dissolved CO_2 in solution in the absence of any protein in solution. (C) Difference spectrum obtained by subtracting the spectrum of freely dissolved CO_2 from CO_2 in the presence of CA II (i.e., A – B). The resulting difference spectrum reveals the IR spectrum of CO_2 bound to CA II. (D) Spectrum of CO_2 in solution in the presence of 7.5 mM wild-type CA II plus 7.5 mM ethoxzolamide. (E) Difference spectrum obtained by subtracting the spectrum of freely dissolved CO_2 from CO_2 in the presence of CA II and inhibitor (i.e., D – B). The resulting difference spectrum reveals that the ethoxzolamide inhibitor successfully blocks CO_2 binding to CA II.

Lipscomb, 1990), and model compound (Woolley, 1975) studies have implicated this region in substrate binding and lowering the pK_a of the zinc solvent molecule. The combination of kinetic and structural measurements leads to an understanding of the accommodation of different amino acids at this position as well as the catalytic function of Leu-198.

Esterase Activity. The esterase activity of CA II is relatively insensitive to substitutions at position 198 with a maximum decrease of 120-fold observed for insertion of a negative charge. With the exception of positively charged (Arg and Lys) and large (Trp) amino acids, esterase activity decreases roughly as the hydrophobicity of the amino acid at residue 198 decreases. The linear correlation of log k_{cat}/K_M versus π (log of the distribution coefficient of acetyl amino acids in octanol/water; Fauchère & Pliska, 1983) (Figure 5) or $\Delta G_R/1.36$ (amino acid solvation energy; Eisenberg & McLachlan, 1986)

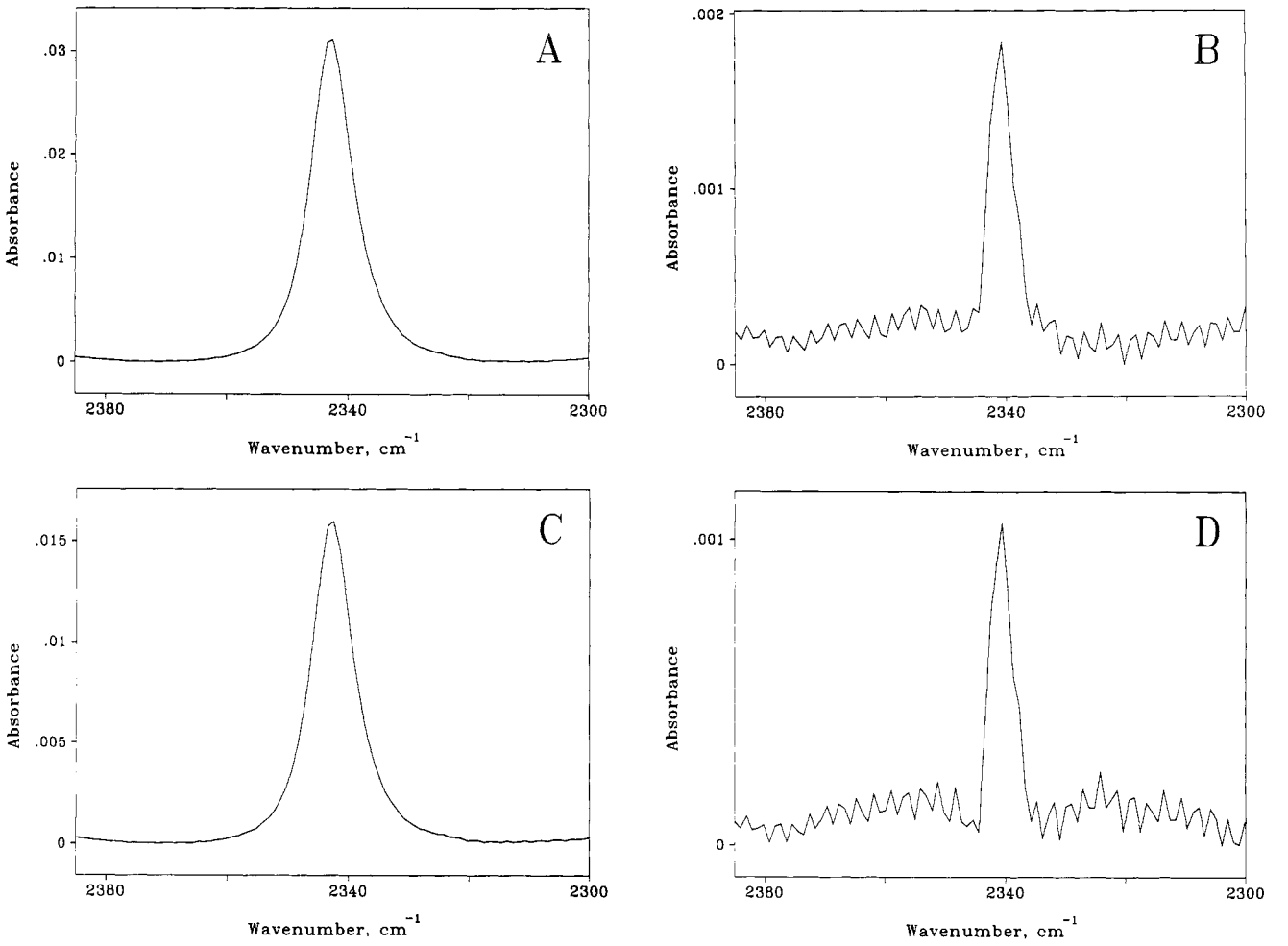

FIGURE 4: Infrared spectra of the asymmetric CO_2 stretching vibration obtained by dissolving CO_2 gas (P_{CO_2} = 1 atm) in 0.25 mM MES, pH 5.5, in the presence of the Leu-198→Arg CA II variant. (A) Spectrum of CO_2 in solution in the presence of 10 mM Leu-198→Arg CA II. (B) Difference spectrum obtained by subtracting the spectrum of freely dissolved CO_2 (Figure 3B) from CO_2 in the presence of 10 mM Leu-198→Arg CA II (i.e., panel A – panel B of Figure 3). The resulting difference spectrum reveals the IR spectrum of CO_2 bound to Leu-198→Arg CA II. (C) Spectrum of CO_2 in solution in the presence of 10 mM Leu-198→Arg CA II plus 10 mM sodium azide. (D) Difference spectrum obtained by subtracting the spectrum of freely dissolved CO_2 (Figure 3B) from CO_2 in the presence of Leu-198→Arg CA II and inhibitor (i.e., panel C – panel B of Figure 3). The resulting difference spectrum reveals that, in this case, CO_2 can bind to the inhibited Leu-198→Arg variant.

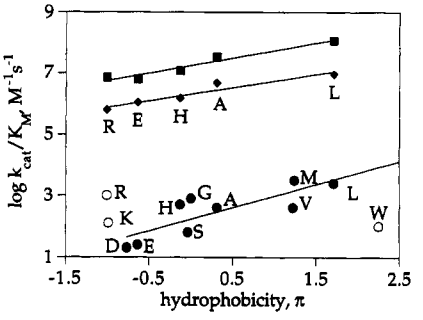

FIGURE 5: Plot of log k_{cat}/K_M for amino acid substitutions at Leu-198 in CA II, measuring either PNPA hydrolysis (○, ●), bicarbonate dehydration (◆), or CO_2 hydration (■) versus hydrophobicity of the substituted amino acid as measured by π [log of the relative distribution coefficient in octanol/water of acetyl amino acids (Fauchère & Pliska, 1983)]. The symbols indicate the substituted amino acid using the one-letter amino acid code. The data (excluding the open symbols) are fit to a line using the fitting program SYSTAT (Systat, Inc.).

gave slopes of 0.76 ± 0.18 (R = 0.83) and 0.8 ± 0.2 (R = 0.81). A similar result was obtained for substitutions at both Val-121 and Val-143 in the hydrophobic pocket (Nair et al., 1991; Fierke et al., 1991). Overall, the results indicate that hydrophobicity stabilizes the transition state for ester hydrolysis relative to the unbound ester, likely due to either charge delocalization in the transition state or desolvation of the zinc hydroxide. In addition, substitution of either lysine or arginine for Leu-198 creates variants that are more active than predicted by their hydrophobicity; perhaps the positive charge stabilizes an anionic tetrahedral transition state similar to that observed in ester hydrolysis by carboxypeptidase (Christianson & Lipscomb, 1989). Finally, although esterase activity is not compromised by a larger active site cavity as indicated by the high activity of Ala substitutions at positions 121, 143, and 198, the decreased activity of the Trp substitution at position 198 and Phe and Tyr substitutions at position 143 is indicative of steric hindrance of the substrate as it approaches the zinc hydroxyl (Nair et al., 1991; Fierke et al., 1991). However, substitution of other amino acids such as His are accommodated by protein rearrangement as observed by X-ray crystallography (Alexander et al., 1991; Nair & Christianson, 1993).

Enzyme pK_a. The pH dependence of esterase activity for wild-type CA II (pK_a ≈6.8) is proposed to reflect the ionization of the zinc–water moiety in the active site (Lindskog, 1966). This value is lower than the ionization of water in many zinc complexes (pK_a of ≈9; Woolley, 1975; Sillèn et al., 1971) but can be modeled by tetracoordinate small molecule complexes (Kimura et al., 1990; Groves & Olson, 1985). Except for Leu-198→Glu, substitution at position 198 causes only

moderate increases (<1 unit) in the pK_a. The observed pH dependence of esterase activity for the Leu-198→Glu variant is parabolic with the activity decreasing upon ionization of either of two groups with apparent pK_as of 5.9 and 8.9. The additional pK_a is likely caused by the ionizable Glu side chain in this mutant which is packed against a hydrophobic surface (Figure 1) (Nair & Christianson, 1993). However, since the pK_as for zinc–water and side-chain carboxylates in hydrophobic environments can be significantly perturbed (Fersht, 1985), the pH dependence is consistent with either of two ionization mechanisms:

$$E_{COOH}^{ZnH_2O} \overset{K_{a1}}{\rightleftharpoons} E_{COOH}^{ZnOH^-} + H^+ \overset{K_{a2}}{\rightleftharpoons} E_{COO^-}^{ZnOH^-} + 2H^+ \quad (5)$$

$$\underset{\text{inactive}}{E_{COOH}^{ZnH_2O}} \overset{K_{a1}}{\rightleftharpoons} \underset{\text{active}}{E_{COO^-}^{ZnH_2O}} + H^+ \overset{K_{a2}}{\rightleftharpoons} \underset{\text{inactive}}{E_{COO^-}^{ZnOH^-}} + 2H^+ \quad (6)$$

Although eq 5 is plausible given the wild-type CA II mechanism, it implies that the Glu substitution significantly decreases the pK_a of the zinc solvent molecule, contrary to simple electrostatic models, and that the pK_a of the carboxylate group is significantly increased due to the hydrophobic environment. In the alternative proposal (eq 6), the pK_a assignments appear more reasonable. However, the mechanism of ester hydrolysis must be altered with the Glu-198 carboxylate group acting as either a nucleophile or general base [as observed in zinc proteases such as carboxypeptidase (Christianson & Lipscomb, 1989)]. A variety of data are consistent with this second mechanism. The pH dependence of the visible spectrum of Co^{2+}-substituted Leu-198→Glu CA II increases with two inflection points consistent with pK_as of about 6 and 9, indicating that ionization of both groups affects the electronic environment of the active site metal (data not shown). The conformation of the Glu side chain in the Leu-198→Glu variant is unchanged as the pH is increased from 8 to 10 (Nair & Christianson, 1993); this is consistent with a pK_a <8 for the carboxylic acid, assuming that ionization would cause movement of the side chain. However, in the X-ray crystal structure [Figure 1; also see Nair and Christianson (1993)] the Glu side chain forms a hydrogen bond with an active site water molecule, not the zinc-bound water molecule as might be expected for a general base-catalyzed mechanism. Nevertheless, the Glu side chain may have enough flexibility to occasionally directly interact with the zinc water, or an active site hydrogen bond network may act as an intermediary. Finally, LoGrasso et al. (1993) have observed that the Phe-198→Asp substitution in CA III causes the zinc–water pK_a to increase from <5 to 9.2.

CO_2 Binding. A previous IR spectroscopic study of bovine carbonic anhydrase (BCA) by Riepe and Wang (1968) suggests that CO_2 binds in a hydrophobic environment in the active site. In the current work involving CA II, we similarly observe a CO_2 difference peak in the IR spectrum of the CO_2-equilibrated enzyme which is shifted to lower wavenumbers when compared to freely dissolved CO_2 in solution (2340 vs 2343.5 cm^{-1}, respectively) (Figure 3). The disappearance of this peak upon the addition of active site inhibitors (sulfonamide or azide) (Vidgren et al., 1990; Nair & Christianson, 1993) indicates that it is caused by CO_2 binding to the active site. The small shift in wavenumbers (3.5 cm^{-1}) indicates that CO_2 is not appreciably strained when bound. However, this wavenumber decrease does indicate that the bound CO_2 residues in a more hydrophobic environment than free, dissolved CO_2 in solution, since the wavenumber peak position of the asymmetric CO_2 stretching vibration decreases with increasing hydrophobicity (Riepe & Wang, 1968).

The intensities of the bound CO_2 band in the [CO_2 + CA II] complex are consistent with a dissociation constant of 100 mM for CO_2, similar to that calculated for BCA (Riepe & Wang, 1968), assuming a 1:1 stoichiometry for the inhibitor-displaceable binding site. This affinity of the zinc–water form of CA II for CO_2 is extremely small, and it is unlikely to increase significantly upon ionization of the zinc water. The K_M for CO_2 hydration is 10 mM, indicating a lower limit for the CO_2 K_D since it mainly reflects a change in rate-limiting steps in the steady-state kinetics (Silverman & Lindskog, 1988). The weak affinity is required for the rapid formation of CO_2 from HCO_3^- reflected in $k_{cat}^{ex} = 2 \times 10^6\ s^{-1}$ (Simonsson et al., 1979), which sets a lower limit for the dissociation rate constant. Given a diffusion-controlled association rate constant of 10^8–$10^9\ M^{-1}\ s^{-1}$ (Eigen & Hammes, 1963) and single-step binding, a minimum K_D of 2–20 mM can be calculated which is smaller than the K_D determined spectroscopically. This weak binding of CO_2 indicates that CA II is an efficient catalyst; the enzyme stabilizes the transition state without "wasting" excessive energy stabilizing the ground-state complex (Jencks, 1975).

The decreased affinity of the inhibitor-displaceable CO_2 binding site to the CA II variant, Leu-198→Arg, combined with the decreased catalytic activity of this variant, further suggests that the IR difference peak at 2340 cm^{-1} reflects CO_2 binding at the active site. This decreased affinity is also observed for the inactive Val-143→Tyr variant (data not shown; Fierke et al., 1991). In addition, the crystal structures of these two mutants (Alexander et al., 1991; Nair & Christianson, 1993; also see Figure 1) indicate that the substituted side chains impinge on the theoretical CO_2 binding site in the hydrophobic pocket shown in Figure 1 (Merz, 1990, 1991; Liang & Lipscomb, 1990), thereby providing experimental confirmation of this site. Interestingly, the Leu-198→Arg mutant decreases the binding of cyanate 8-fold (Krebs and Fierke, unpublished data), which is proposed to mimic the binding of CO_2 to the active site (Lindahl et al., 1993). In wild-type human CA II there is no evidence for additional binding sites. However, a CO_2 peak that is not displaceable by azide is observed for the Leu-198→Arg mutant, indicating that the position of CO_2 binding is altered [since the azide binding mode is unchanged (Nair & Christianson, 1993)], perhaps reflecting alternative CO_2 binding sites (Merz, 1990, 1991; Liang & Lipscomb, 1990).

CO_2 and HCO_3^- Interconversion. In addition to decreasing CO_2 binding, substitutions at Leu-198 cause significant decreases in k_{cat} and k_{cat}/K_M for both CO_2 hydration and HCO_3^- dehydration. These effects may best be interpreted in the context of the accepted catalytic mechanism (Silverman & Lindskog, 1988). There is considerable evidence that hydration of CO_2 by CA II consists of two steps: CO_2/HCO_3^- interconversion involving the metal center (eq 7) followed by a proton-transfer step involving a "proton-shuttle" group (proposed to be the His-64 side chain) and containing a buffer-dependent reaction (eq 8).

$$E\text{–}OH^- + CO_2 \overset{k_1}{\underset{k_{-1}}{\rightleftharpoons}} E\text{–}OH^-\cdot CO_2 \overset{k_2}{\underset{k_{-2}}{\rightleftharpoons}} E\text{–}HCO_3^- \overset{k_3[H_2O]}{\underset{k_{-3}}{\rightleftharpoons}} E\text{–}OH_2 + HCO_3^- \quad (7)$$

$$E\text{–}OH_2 \overset{k_4}{\underset{k_{-4}}{\rightleftharpoons}} {}^+H\text{–}E\text{–}OH^- \overset{k_5[B]}{\underset{k_{-5}[BH^+]}{\rightleftharpoons}} E\text{–}OH^- \quad (8)$$

The second-order rate constant, k_{cat}/K_M, is only a function of the rate constants up to and including product release (eq 7) but not proton transfer (eq 8). For wild-type CA II the pH-independent $k_{cat}^{CO_2}/K_M = k_1k_2k_3/(k_2k_3 + k_{-1}k_3 + k_{-1}k_{-2}) \approx k_1k_2/k_{-1}$ and $k_{cat}^{HCO_3^-}/K_M = k_{-1}k_{-2}k_{-3}/(k_2k_3 + k_{-1}k_3 + k_{-1}k_{-2}) \approx k_{-2}k_{-3}/k_3$ because $k_{-2} < k_3$ (Lindskog, 1984; Rowlett, 1984) and $k_{-1} \geq k_2$ since the viscosity dependence of $k_{cat}^{CO_2}/K_M$ suggests that this parameter does not attain the diffusion-control limit (Pocker & Janjić, 1987). Therefore, k_{cat}/K_M in either direction reflects the transition state for CO_2/HCO_3^- interconversion in wild-type CA II. The observation that log k_{cat}/K_M for both directions is linearly related to the hydrophobicity of the side chain (Figure 5) as measured by either π (Fauchère & Pliska, 1983) or $\Delta G_R/1.36$ (Eisenberg & McLachlan, 1986) with slopes for CO_2 hydration of 0.5 (R = 0.97) and 0.41 (R = 0.86), respectively, and for HCO_3^- dehydration of 0.44 (R = 0.96) and 0.41 (R = 0.91), respectively, suggests that these simplifications are also applicable to the mutants. These are higher correlations than observed for $k_{cat}^{CO_2}/K_M$ with similar substitutions at position 198 in CA III; in this case bicarbonate dissociation is partially rate-limiting (LoGrasso et al., 1993). The effect of hydrophobicity on CO_2/HCO_3^- interconversion may suggest that the transition state is less polarized (or has greater dispersion of electron density) than the ground state composed of CA II and unbound substrate. Finally, the observation of a solvent isotope effect in $k_{cat}^{HCO_3^-}/K_M$ for the Leu-198→Ala mutant indicates either a change in the rate-limiting step or a change in the mechanism; perhaps an internal proton transfer in zinc-bound bicarbonate, proposed by Liang and Lipscomb (1987), becomes kinetically significant.

At saturating substrate concentrations the observed rate constant, k_{cat}, is a function of both CO_2/HCO_3^- interconversion and proton transfer (eqs 7 and 8). A significant solvent isotope effect on $k_{cat}^{CO_2}$ is observed for all substitutions, indicating that k_4, the intramolecular proton transfer from zinc–water to His-64, is a significant rate-contributing step. Analogously, k_{-4} is the rate-limiting step for HCO_3^- dehydration for wild-type and Leu-198→Ala CA II. The solvent isotope effect on $k_{cat}^{HCO_3^-}$ disappears for the Leu-198→Glu and Leu-198→Arg variants, indicating that one of the interconversion steps (eq 7) is rate-limiting; hence, $k_{cat}^{HCO_3^-} = k_{-1}k_{-2}/(k_2 + k_{-2} + k_{-1})$. For the Leu-198→Arg variant, this measurement most likely reflects k_{-2} since CO_2 binding decreases and a solvent isotope effect is observed for CO_2 hydration. Furthermore, the steady-state and equilibrium kinetic measurements [$K_{eff}^{HCO_3^-}$ = 47 mM (Leu-198→Arg) versus 150 mM (wild-type) at pH 7 (Simonsson et al., 1979)] indicate that HCO_3^- binding does not decrease and may actually increase compared to wild type. Therefore, the introduction of a positive charge at this position stabilizes the E·HCO_3^- complex and destabilizes the transition state for dehydration.

The intramolecular proton transfer from zinc–H_2O to His-64 is both increased (Leu-198→Ala) and decreased significantly (Leu-198→Arg) by substitutions at position 198; this was not observed for mutations at other residues in the hydrophobic pocket (Nair et al., 1991; Fierke et al., 1991). Since the transfer is proposed to occur via water molecules (Eriksson, 1988; Venkatasubban & Silverman, 1980), these effects are likely mediated by the changes in the active site water structure observed in the crystallographic studies of these mutations (Nair & Christianson, 1993). Previous structure–function studies of the Thr-200→Ser mutant of CA II indicated that proton transfer is unaffected by the side-chain conformation of His-64 (Krebs et al., 1991). However, the increased pK_a for His-64 in the Leu-198→Ala mutant [indicated by the elevated observed pK_a for $k_{cat}^{CO_2}$ (Simonsson et al., 1979)] makes the transfer of a proton from zinc–H_2O to His-64 more thermodynamically favorable, and this may be reflected in the increased rate constant.

Comparison to CA III. The low catalytic activity and decreased inhibitor binding of CA III isozymes are proposed to result from blockage of the active site by the Phe-198 side chain present in this isozyme (Eriksson, 1988). LoGrasso et al. (1991) have demonstrated that the properties of the Phe-198→Leu variant of CA III are similar to CA II; k_{cat}/K_M for both CO_2 hydration and *p*-nitrophenyl acetate hydrolysis increases, the pK_a for the zinc-bound water increases, and sulfonamide binding increases. However, substitution of Phe for Leu-198 in CA II has little or no effect on the catalytic properties (Ren et al., 1991). This difference can be rationalized by the varied side-chain conformation in the two isozymes. The X-ray crystal structure of the Leu-198→His variant (Nair & Christianson, 1993) indicates that the His side chain, and likely the Phe side chain as well, packs against a hydrophobic surface (formed by residues Pro-202, Phe-131, Leu-141, and Leu-204) enlarging the hydrophobic pocket. In bovine CA III, the Phe-198 side chain points into the active site, decreasing the volume of the pocket (Eriksson, 1988). This difference may be mediated by substitutions in the hydrophobic surface of bovine CA III including Leu-141→Ile and Leu-204→Glu. Substitutions of other amino acids at position 198 also lead to differing properties in CA II compared to CA III (LoGrasso et al., 1993), which are probably due to varied side-chain positions as well.

ACKNOWLEDGMENT

We thank L. L. Kiefer, S. K. Nair, and D. W. Christianson for helpful discussions and Y.-Y. Shin for preparing cobalt-substituted enzymes. We thank N. B. Tweedy and the Duke University Graphics Center for help with preparing figures and interpreting the structural data.

REFERENCES

Alexander, R. S., Nair, S. K., & Christianson, D. W. (1991) *Biochemistry 30*, 11064–11072.

Armstrong, J. M., Myers, D. V., Verpoorte, J. A., & Edsall, J. T. (1966) *J. Biol. Chem. 241*, 5137–5149.

Bertini, I., Canti, G., Luchinat, C., & Borghi, E. (1983) *J. Inorg. Biochem. 18*, 221–229.

Bertini, I., Luchinat, C., Monnanni, R., Roelens, S., & Moratal, J. M. (1987) *J. Am. Chem. Soc. 109*, 7855–7856.

Brion, L. P., Schwartz, J. H., Zavilowitz, B. J., & Schwartz, G. J. (1988) *Anal. Biochem. 175*, 289–297.

Cameron, D. G., Casal, H. L., & Mantsch, H. H. (1979) *J. Biochem. Biophys. Methods 1*, 21–36.

Cameron, D. G., Kauppinen, J. K., Moffat, D., & Mantsch, H. H. (1982) *Appl. Spectrosc. 36*, 245–250.

Christianson, D. W. (1991) *Adv. Protein Chem. 42*, 281–355.

Christianson, D. W., & Lipscomb, W. N. (1989) *Acc. Chem. Res. 22*, 62–69.

Coleman, J. E. (1967) *J. Biol. Chem. 242*, 5212–5219.

D'Esposito, L., & Koenig, J. L. (1978) in *Fourier transform infrared spectroscopy: applications to chemical system* (Ferraro, J., & Basile, L., Eds.) Academic Press, New York.

Eigen, M., & Hammes, G. G. (1963) *Adv. Enzymol. Relat. Subj. Biochem. 25*, 1–38.

Eisenberg, D., & McLachlan, A. D. (1986) *Nature 319*, 199–203.

Eriksson, A. E., Jones, T. A., & Liljas, A. (1986) in *Zinc Enzymes* (Bertini, I., Luchinat, C., Maret, W., & Zeppezauer, M., Eds.) pp 317–328, Birkhauser, Boston, MA.

Eriksson, A. E., Kylsten, P. M., Jones, T. A., & Liljas, A. (1988) *Proteins: Struct., Funct., Genet. 4*, 283–293.
Fauchère, J. L., & Pliska, V. (1983) *Eur. J. Med. Chem. 18*, 369–375.
Fersht, A. R. (1985) *Enzyme Structure & Mechanism*, 2nd ed., pp 172–174, W. H. Freeman & Co., New York.
Fierke, C. A., Calderone, T., & Krebs, J. F. (1991) *Biochemistry 30*, 11054–11063.
Glasoe, P., & Long, F. (1960) *J. Phys. Chem. 64*, 188–190.
Groves, J. T., & Olson, J. R. (1985) *Inorg. Chem. 24*, 2715–2717.
Håkansson, K., Carlsson, M., Svensson, L. A., & Liljas, A. (1992) *J. Mol. Biol. 227*, 1192–1204.
Hanahan, D. (1983) *J. Mol. Biol. 166*, 557–580.
Hewett-Emmett, D., & Tashian, R. E. (1991) in *Structure and evolutionary origins of the carbonic anhydrase multigene family* (Dodgson, S. J., Tashian, R. E., Gros, G., & Carter, N. D., Eds.) pp 15–32, Plenum Press, New York.
Jencks, W. P. (1975) *Adv. Enzymol. Relat. Areas Mol. Biol. 43*, 219–410.
Khalifah, R. G. (1971) *J. Biol. Chem. 246*, 2561–2573.
Kimura, E., Shiota, T., Koike, T., Shiro, M., & Kodama, M. (1990) *J. Am. Chem. Soc. 112*, 5805–5811.
Krebs, J. F., & Fierke, C. A. (1993) *J. Biol. Chem. 268*, 948–954.
Krebs, J. F., Alexander, R. F., Christianson, D. W., & Fierke, C. A. (1991) *Biochemistry 30*, 9153–9160.
Liang, J.-Y., & Lipscomb, W. N. (1987) *Biochemistry 26*, 5293–5301.
Liang, J.-Y., & Lipscomb, W. N. (1990) *Proc. Natl. Acad. Sci. U.S.A. 87*, 3675–3679.
Liljas, A., Kannan, K. K., Bergstén, P.-C., Waara, I., Fridborg, K., Strandberg, B., Carlbom, U., Järup, L., Lövgren, S., & Petef, M. (1972) *Nature (London), New Biol. 235*, 131–137.
Lindahl, M., Svensson, A., & Liljas, A. (1993) *Proteins: Struct., Funct., Genet. 15*, 177–182.
Lindskog, S. (1966) *Biochemistry 5*, 2641–2646.
Lindskog, S. (1984) *J. Mol. Catal. 23*, 357–368.
Lindskog, S., & Coleman, J. E. (1973) *Proc. Natl. Acad. Sci. U.S.A. 70*, 2505–2508.
LoGrasso, P. V., Tu, C. K., Jewell, D. A., Wynns, G. C., Laipis, P. J., & Silverman, D. N. (1991) *Biochemistry 30*, 8463–8470.
LoGrasso, P. V., Tu, C., Chen, X., Taoka, S., Laipis, P. J., & Silverman, D. N. (1993) *Biochemistry* (in press).
Merz, K. M., Jr. (1990) *J. Mol. Biol. 214*, 799–802.
Merz, K. M., Jr. (1991) *J. Am. Chem. Soc. 113*, 406–411.
Nair, S. K., & Christianson, D. W. (1993) *Biochemistry* (following paper in this issue).
Nair, S. K., Calderone, T. L., Christianson, D. W., & Fierke, C. A. (1991) *J. Biol. Chem. 266*, 17320–17325.
Osborne, W. R. A., & Tashian, R. E. (1975) *Anal. Biochem. 64*, 297–303.
Pocker, Y., & Stone, J. T. (1967) *Biochemistry 6*, 668–678.
Pocker, Y., & Janjić, N. (1987) *Biochemistry 26*, 2597–2606.
Ren, X. L., Jonsson, B. H., & Lindskog, S. (1991) *Eur. J. Biochem. 201*, 417–420.
Riepe, M. E., & Wang, J. H. (1968) *J. Biol. Chem. 243*, 2779–2787.
Rowlett, R. S. (1984) *J. Protein Chem. 3*, 369–393.
Sanger, F., Nicklen, S., & Coulson, A. R. (1977) *Proc. Natl. Acad. Sci. U.S.A. 74*, 5463–5467.
Showen, R. L. (1977) in *Isotope Effects on Enzyme Catalyzed Reactions* (Cleland, W. W., O'Leary, M. H., & Northrup, D. B., Eds.) pp 64–99, University Park Press, Baltimore, MD.
Sillèn, L. G. (1964) *Stability constants of metal ion complexes*, 2nd ed., The Chemical Society, London.
Silverman, D. N., & Lindskog, S. (1988) *Acc. Chem. Res. 21*, 30–36.
Simonsson, I., Jonsson, B. H., & Lindskog, S. (1979) *Eur. J. Biochem. 93*, 409–417.
Stanssens, P., Opsomer, C., McKeown, Y. M., Kramer, W., Zabeau, M., & Fritz, H.-J. (1989) *Nucleic Acids Res. 17*, 4441–4454.
Steiner, H., Jonsson, B. H., & Lindskog, S. (1975) *Eur. J. Biochem. 59*, 253–259.
Studier, F. W., & Moffatt, B. A. (1986) *J. Mol. Biol. 189*, 113–130.
Thomas, G. J., Jr., & Kyogoku, Y. (1977) in *Infrared and Raman spectroscopy* (Brame, E. A., Jr., & Grasselli, J. A., Eds.) Vol. 1, Marcel Dekker, Inc., New York.
Tu, C. K., & Silverman, D. N. (1982) *Biochemistry 21*, 6353–6360.
Tu, C. K., Silverman, D. N., Forsman, C., Jonsson, B. H., & Lindskog, S. (1989) *Biochemistry 28*, 7913–7918.
Venkatasubban, K. S., & Silverman, D. N. (1980) *Biochemistry 19*, 4984–4989.
Vidgren, J., Liljas, A., & Walker, N. P. C. (1990) *Int. J. Biol. Macromol. 12*, 342–344.
Williams, T. J., & Henkens, R. W. (1985) *Biochemistry 24*, 2459–2462.
Woolley, P. (1975) *Nature 258*, 677–682.